FATIGUE STRENGTH OF WELDED TUBULAR T-JOINTS MADE OF FERRITIC STAINLESS STEEL IN AS-WELDED AND POST-WELD TREATED CONDITION

MATTI KOSKIMÄKI[a], NIKO TUOMINEN[b], ANTTI AHOLA[c] and TIMO BJÖRK[d]

Laboratory of Steel Structures, Lappeenranta-Lahti University of Technology LUT, Yliopistonkatu 34, FI-53850, Lappeenranta, Finland.

E-mail: [a]matti.koskimaki@lut.fi, [b]niko.tuominen@lut.fi, [c]antti.ahola@lut.fi, [d]timo.bjork@lut.fi

In the present study, fatigue tests were carried out for welded thin-walled tubular T-joints made of the ferritic stainless steel 1.4003. The specimens were prepared using gas metal arc welding. The fatigue tests were performed using fully reverse (R = -1) in-plane bending loading, at the intermediate regime, i.e. resulting in 10^5–10^6 cycles in fatigue life. The T-joints were tested in as-welded (AW), tungsten inert gas (TIG)-dressed and high frequency mechanical impact (HFMI)-treated condition. Fatigue strength assessment was conducted using the effective notch stress (ENS) concept with r_{ref} = 0.05 mm reference radius and FAT630 curve, as recommended for the plate thicknesses less than 5 mm, showing a good agreement with the experimental results. According to the fatigue test results, 1.3–1.4 improvement in fatigue strength can be claimed when applying post-weld treatments. Use of robotic welding, instead of manual welding, resulted in slightly higher fatigue strength in the joints in the AW condition.

Keywords: *Ferritic stainless steel, tubular structures, welded joints, fatigue strength, post-weld treatment;*

1 Introduction

Tubular members are widely used due to their good structural performance. The hollow cross section obtains good or even excellent capacities for different loading cases. The applications cover may kind of structures subjected both static and fluctuating loads (Packer et al. 2009). Nowadays, several material options are available for different loading conditions and environmental needs. Fatigue strength properties of tubular joints made C-Mn steels can be found in prior studies (van Wingerde 1992). However, designers lack of design data concerning the strength properties of welded tubular joints made of stainless steel. There exist published results related to fatigue strength of welded joints made of different stainless steels in as-welded (AW) or post-weld treated (PWT) condition (Maddox and Manteghi 2002; European Commission 2007; Björk et al. 2018). Furthermore, ferritic stainless steels (FSSs) in welded components have shown good fatigue strength properties with respect to fatigue strength properties of base metal (Akita et al. 2018) and other stainless steel materials (Niemi and Koskimäki 1997). However, fatigue design data concerning welded tubular joints made of FSS is not available. Such ferritic tubes are widely used e.g. as material in bus chassis and consequently, there are high requirements for weight of the construction and quality of joints. The present paper introduces an experimental fatigue test program conducted on the tubular joints made of thin-walled (t = 2 mm) FSS rectangular hollow sections (RHSs). The specimens were tested in the AW, tungsten inert gas (TIG)-dressed and high frequency mechanical impact

Proceedings of the 17th International Symposium on Tubular Structures.
Editors: X.D. Qian and Y.S. Choo

Published by Research Publishing, Singapore.
ISBN: 978-981-11-0745-0; doi:10.3850/978-981-11-0745-0_056-cd

(HFMI)-treated condition. Numerical analyses were carried out to investigate the applicability of effective notch stress (ENS) concept (Sonsino et al. 2012), for the thin-walled tubular structures.

2 Experimental fatigue tests

2.1 *Materials*

The RHS tubes were fabricated from a ferritic stainless steel 1.4003 (EN 10088-2 2014). Two matching filler metals were used: Esab OK Autrod 316LSi (G 19 12 3 LSi, denoted with FM1), and Elga Cromamig 308LSi (G 19 9 L Si, denoted with FM2) after EN ISO 14343 (2017), as seen in Table 1. It is worth noting that the actual values of mechanical properties in the joints of the RHS members depend on degree of cold-forming and welding heat input and consequently, might differ from the presented values.

Table 1. Mechanical properties and chemical composition of the studied materials. BM is the base material (1.4003), $R_{p0.2}$ and R_m are the yield and ultimate strength of material, respectively, A_5 uniform elongation and KV impact energy at the 20°C temperature.

	Mechanical properties (minimum values)				Chemical composition (weight-%) (maximum values)								
ID	$R_{p0.2}$ (MPa)	R_m (MPa)	A_5 (%)	KV (J)	C	Si	Mn	P	S	N	Cr	Ni	Mo
BM	320	450	10	-	0.03	1.0	1.5	0.04	0.015	0.03	12.5	1.0	-
FM1	440	620	37	120	0.02	0.8	1.8	-	-	-	18.5	12	2.8
FM2	400	590	40	120	0.02	0.8	1.75	-	-	-	20.0	10	-

2.2 *Specimen preparation*

The T-joints, shown in Figure 1a, were prepared by welding tubular RHSs (60 × 40 × 2 mm) with gas metal arc welding (GMAW) process. The industrial cooperative partner welded the vast majority of the specimens and conducted also the TIG dressing in the selected specimens. The specimens prepared with a robotic welding (see AWL1-AWL3, Table 3 in Section 2.5), were welded with two run-on/run-off positions located at the wider side on the brace member. Respectively, manually welded specimens had four run-on/run-off positions at the end of groove on the chord face, still avoiding positioning them at the corner area. The welding parameters were: voltage U = 24.4 V, current I = 160 A, travel speed v_{travel} = 24 cm/min, and Ar+2%O_2 was used as a shielding gas. The applicability of the welding parameters was confirmed by a preliminary pre-production welding test that was also an approval test for pre-welding procedure specification (pWPS). The most important criterion for welding quality was the adequate throat thickness without lack of fusion-type of flaws.

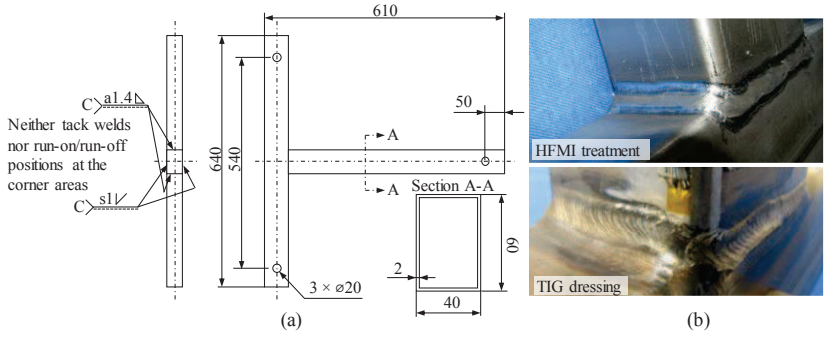

Figure 1. (a) Specimen dimensions, and (b) examples on PWTs

In selected specimens, PWTs were carried out using the HFMI treatments and TIG dressing, see Fig 1b and Table 3 that summarizes the test matrix (Section 2.5). The treatment is needed only at the highly stressed corner areas of the joint but considering the size of joints and weldments, all weld toes were treated.

2.3 *Measurements*

To define weld geometry (throat thickness and weld toe radius), macro sections were chosen from typical specimen representing each series. The results of the analyses are presented in Table 2. Surface residual stress measurements were performed by X-ray diffractometer (Stresstech X3000 G3). Residual stresses were measured at the corner and the middle of the side walls of the chord and brace, as shown in Fig. 2a. Residual stresses were measured in the joints in the AW condition and after the HFMI treatment. The measurements were repeated using a 1 mm pitch and starting from the weld toe line. The results of the measurements can be found in Fig. 2b.

Table 2. Results of geometry measurements. a is the throat thickness and r_{true} is the weld toe radius

Joint condition	Specimen ID	a (mm)	r_{true} (mm)
AW	AWR15	3.1-3.4	0.2-1.0
	AWL1	4.1-4.3	0.4-3.9
	AWK9	2.7-3.0	0.2-1.4
TIG	1S	2.9-3.2	7.4-14.6
	1SJ	3.0-3.5	0.7-5.7
HFMI	UP2	3.3-3.5	1.07-1.82

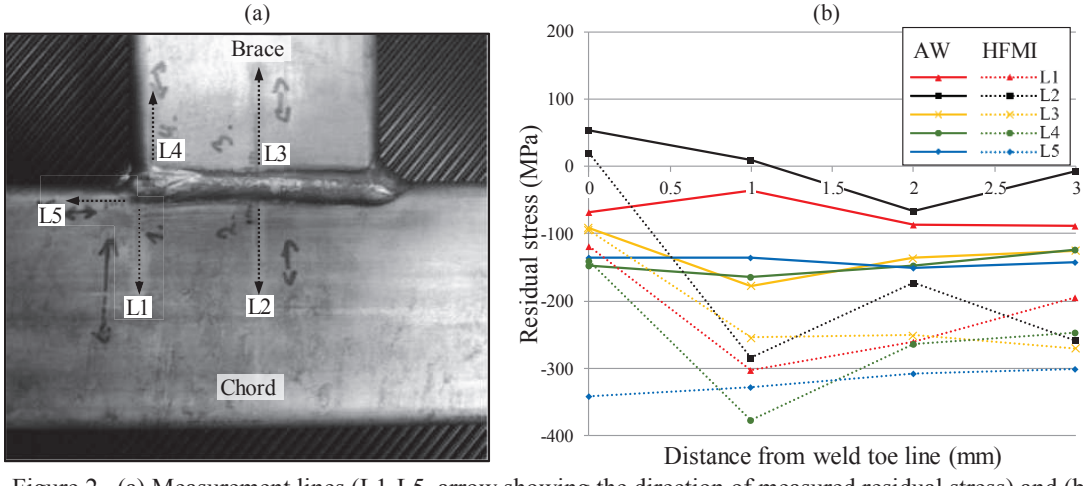

Figure 2. (a) Measurement lines (L1-L5, arrow showing the direction of measured residual stress) and (b) results of residual stress measurements.

2.4 *Test set-up*

The constant amplitude loading (CAL) fatigue tests were performed using two different test set-ups: the conventional tests with servo-hydraulic actuator (Fig. 3a), and using a rotating eccentric mass vibrator (Fig. 3b). In both tests, the boundary conditions were similar, expect for the vibration tests, an additional pin was added to the center of the chord member to avoid undesirable vibration modes, such as the vertical vibration of the chord member and the out of plane vibration of the brace member. In the vibration tests, due to the boundary conditions and

stiffness of test specimen, the lowest frequency is in-plane waiving mode representing nearly pure fully reverse bending moment loading in the investigated joint and consequently, the stress ratio was $R = S_{min}/S_{max} = M_{min}/M_{max} = -1$. The frequency of the vibrator during the fatigue tests was approximately 30 Hz, depending of system's natural frequency and desired strain range. Failure criterion to interrupt the fatigue test was a 25% increase in displacement measured 400 mm far from the joint, see the displacement transducer in Fig. 4a.

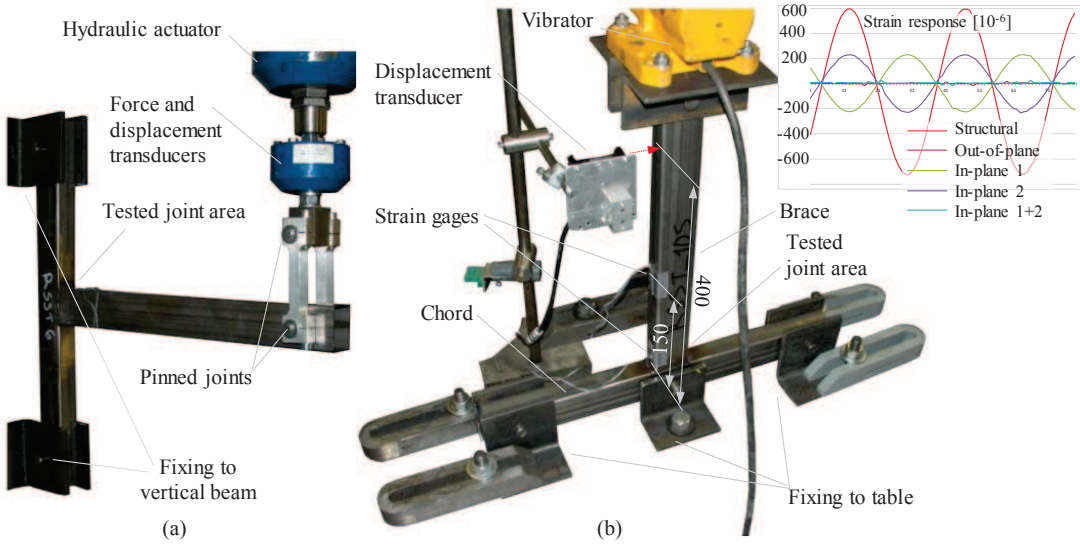

Figure 3. Test set-ups used in the fatigue tests: (a) servo-hydraulic and vibration test set-up with strain response measured from the strain gages. Structural strain range correspond to the gage located next to the weld.

The nominal strains, 150 mm far from the weld toe, as shown in Fig 3a, were measured in the first tests in order to calibrate and verify a proper behavior of the vibrating load system. In addition, one strain gage was installed at the web (60 mm side) of the brace member to identify the out-of-plane bending behavior of the system. The strain gage values distinguished less than 2% from the values from the values produced in the servo-hydraulic tests. In-plane displacement, at the 400 mm distance from the joint in the brace member, was recorded during the tests. The measurements (minimum and maximum values) were recorded with a 1-minute interval during fatigue tests.

In addition to the vibration-based fatigue tests, four comparative fatigue tests were conducted using a servo-hydraulic material testing machine, Figure 4b. The boundary conditions were similar to the vibration tests, except no fixing at the middle of the chord was needed. The loading rate was (only) 0.6 Hz in the servo-hydraulic tests.

2.5. *Fatigue test results*

Fatigue test results are seen in Table 3 and Fig. 4 presents S-N curves determined based on the IIW recommendations (Hobbacher 2016).

Table 3. Fatigue test results.

AW specimens					TIG-dressed specimens					HFMI-treated specimens				
ID[1]	Rig[2]	ΔM (kNm)	$N_{f,exp}$ (cycles)	F[3]	ID[1]	Rig[2]	ΔM (kNm)	$N_{f,exp}$ (cycles)	F[3]	ID[1]	Rig[2]	ΔM (kNm)	$N_{f,exp}$ (cycles)	F[3]
AWR1	V	1.038	696 385	CT	1S	V	1.670	447 649	BT	UP2	V	1.349	1 147 981	R
AWR3	V	1.325	266 693	CT	2S	V	1.317	1 140 029	BT	UP4	V	1.645	671 994	R
AWR5	V	1.687	129 829	CT	3S	V	1.666	273 942	BT	UP7	V	1.576	501 097	R
AWR6	H	1.638	97 891	CT	4S	V	1.309	998 515	CT	UP9	V	1.611	313 227	BM
AWR8	H	1.539	161 078	BT	5S	V	1.699	427 697	BT	UP10	V	1.313	1 115 833	R
AWR11	H	1.427	179 185	CT	6S	V	1.299	399 782	BT	UP12	H	1.337	951 583	R
AWR14	V	1.206	908 939	BT	7S	V	1.289	1 109 328	BT	UP13	V	1.669	907 126	CT
AWR15	V	1.117	880 925	BT	8S	V	1.296	992 754	BT	UPL1	V	2.220	165 161	R
AWL1	V	1.658	212 404	CT	9S	V	1.659	546 489	BT	UPL2	V	2.406	138 555	BT
AWL2	V	1.844	154 282	CT	10S	V	1.667	408 644	BT	UPL3	V	2.408	111 776	BM
AWL3	V	1.946	74 030	CT	1SJ	V	1.673	385 884	BT					
AWK1	V	1.289	445 961	CT	2SJ	V	1.827	309 861	BT					
AWK2	V	1.679	115 279	BT	3SJ	V	2.210	119 424	BT					
AWK3	V	1.697	83 049	CT										
AWK4	V	1.272	368 777	CT										
AWK5	V	1.308	292 885	CT										
AWK6	V	1.672	87 099	BT										
AWK7	V	1.659	143 135	CT										
AWK8	V	1.112	561 557	BT										
AWK9	V	1.664	141 391	CT										
AWK10	V	1.654	126 971	CT										

[1]Specimen ID notation:
Joint condition: AW = as-welded, S = TIG-dressed, UP = HFMI-treated
Joint fabrication: R = industrial partner 1 (manual welding), L = fabricated at LUT (robotic welding), K = industrial partner 2 (manual welding). Additional tests in the series denoted with 'J'
[2]Test rig: V = Vibration test, H = servo-hydraulic test
[3]Failure location: CT = weld toe of chord member, BT = weld toe of brace member, R = weld root failure, BM = base material of chord member

In the statistical analyses, the AW specimens AW14, AW15, AWL1, AWL2, AWL3, and the TIG-dressed specimen 6S were excluded since they diverge distinctly from the other test results in the series, as shown in Fig. 4. The stress range is defined on basis of nominal stress at the brace and chord connection. Although the nominal stress at the welded detail is unambiguous, it can be used here for comparison, because the joint dimensions are the same for all test specimens. Fig. 5 shows the typical failure modes occurred at the specimens.

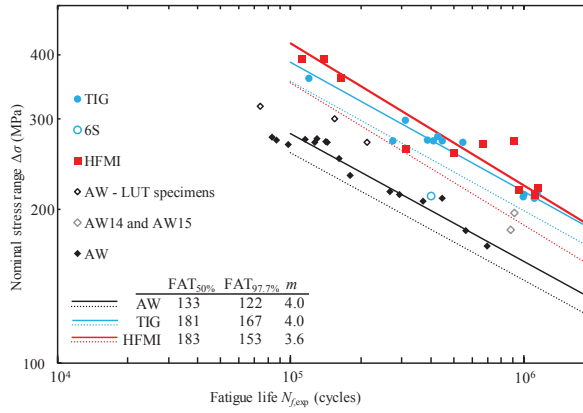

Figure 4. Fatigue test results in terms of nominal stress system, calculated on the basis the moment range and section modulus of the brace member (see further details in Table 3).

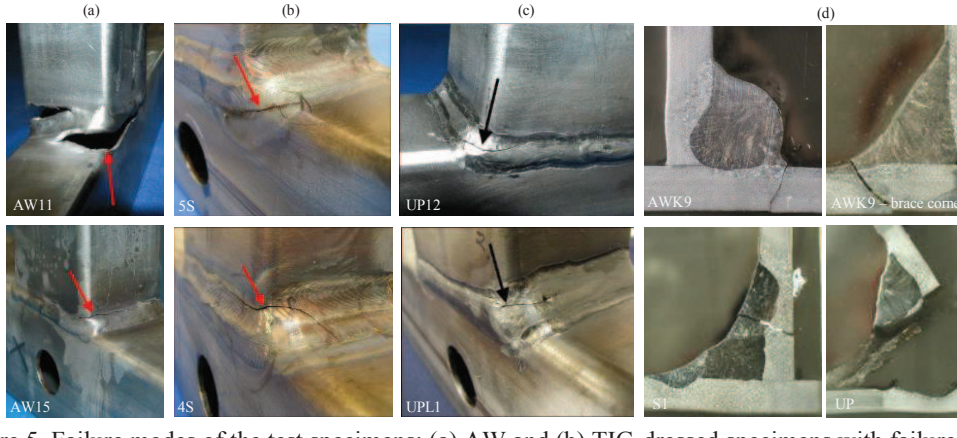

Figure 5. Failure modes of the test specimens: (a) AW and (b) TIG-dressed specimens with failures at the weld toe of brace member (AW11, 5S) and at the weld toe of chord member (AW15, 4S), and weld root failures in the HFMI-treated specimens (UP12, UPL1), (d) macro sections of failed specimens.

3 Fatigue strength assessment using effective notch stress (ENS) concept

A 3D solid element FE-model was created to investigate the computational fatigue strength of the joint using the ENS concept. The reference radius of r_{ref} = 0.05 mm was used in the model, as recommended for the plate thicknesses less than 5 mm (Sonsino et al. 2012). Currently, r_{ref} = 0.05 mm with FAT630 reference S-N curve is available only for joints in the AW condition and consequently, these analyses focused on the tested AW specimens. As the ENS approach requires high mesh density at the critical details, sub-modeling technique with 20-noded hexahedral elements was employed to reduce the computational time needed for the analyses, see Fig. 6a-b. The weld profile was modeled following the worst profile found in macrographic investigations, see Fig. 5d, and the RHS profiles were modeled using the nominal dimensions. Steel material with Young's modulus E = 210 GPa and Poisson's ratio v = 0.3 was used in the analyses. All analyses were carried out using the commercial ABAQUS software applying M = 0.8 kNm moment load resulting in an ENS of σ_{ens} = 1925 MPa that was used as a basis for the fatigue strength estimations.

In Fig. 6c, the fatigue test data points are presented in terms of the ENS concept with respect to the FAT630 reference curve. The test data indicated shallower slope than the

reference curve but the fatigue strengths (mean representing 50% and char 97.7% survival probability) were obtained also for the fixed slope of $m = 3$, showing a good accordance with the reference curve.

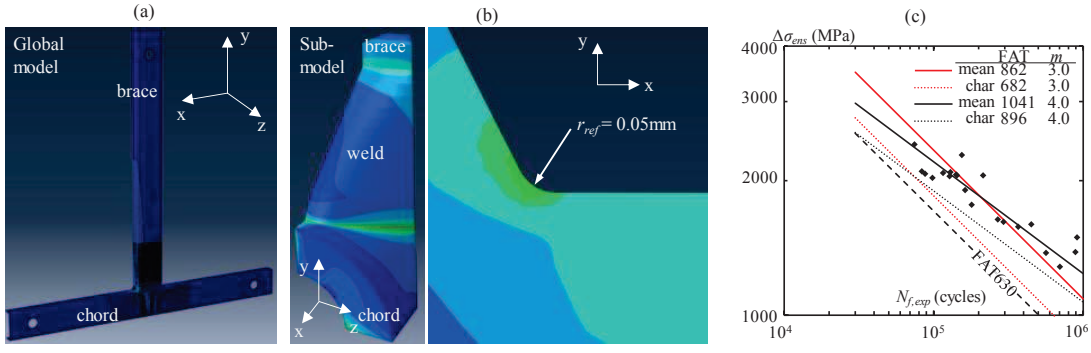

Figure 6. ENS-based FE-model used in the analyses: (a) global model and (b) sub-model at the corner area, and (c) S-N curves in terms of the ENS concept.

4 Discussion and conclusions

In the present study, an extensive experimental fatigue test program, and numerical analyses were carried out to investigate the fatigue performance of FSS tubular joints made of thin-walled RHSs. Fatigue tests were conducted with the CAL with applied stress ratio of $R = -1$ using two different test set-ups: vibration and servo-hydraulic tests, see Fig. 2. No differences were found between the results obtained by the vibration and servo-hydraulic tests were found, indicating the potential of use of vibration-based systems in such fatigue tests. With robotic welding, an increase in fatigue strength was found with respect to the manually welded specimens, see Fig. 4, likely due to the constant welding quality around the corner of brace member and higher weld toe radius, see Table 2 and Table 3.

TIG dressing and HFMI treatment were considered as PWT methods to improve the fatigue strength of the joint. The results showed that approximately 1.3-1.4 improvement in the fatigue strength can be claimed when using PWTs, see Fig. 4, verifying the applicability of the PWT improvement factors introduced by Haagensen and Maddox (2010). Nevertheless, it must be noted that in the case of the HFMI-treated joints, the fatigue failures occurred at the weld root, see Fig. 5d and Table 3, and thus the full potential of the treatment could not be reached. Due to the weld root failures in the HFMI-treated joints, steeper S-N curve slope ($m = 3.6$) was obtained with respect to the AW and TIG-dressed joints for which $m = 4.0$ was obtained. For TIG-dressed joints, $m = 4$ has been suggested also by Yıldırım (2017) and Skriko et al. (2017). Due to the small weld size, the TIG dressing in the studied joints can be regarded as weld treatment, not as weld toe treatment, like originally intended. In some specimens, this resulted unsuccessfully in severe weld toe radii, as shown in Table 2.

Numerical analyses following the ENS concept were carried out using the artificial reference radius of $r_{ref} = 0.05$ mm in a 3D geometry representing the worst-case weld geometry in the AW test series. The pre-processing of the complex weld geometry around the brace member, i.e. weld profile changes from fillet weld to almost butt weld, was found difficult, see the geometry in Fig. 6b. The analyses, however, resulted in good agreement with the FAT630 design curve recommended for the plate thicknesses less than 5 mm, as shown in Fig 6d. Nevertheless, considering the applied stress ratio of external loading ($R = -1$, mean stress $S_{mean} = 0$) used in the fatigue tests, and low tensile or even compressive residual stresses measured in the joint in the AW condition, further verification should be thus conducted for higher mean stress

levels. Based on the experimental tests and numerical analyses, the following conclusions can be drawn:

- The fatigue strength of tubular joints, made of FSS material, was equal or even better than counterparts made of structural or stainless steel;
- TIG dressing, and particularly HFMI treatment showed their potential as fatigue strength improvement techniques, also for the studied thin-walled RHS joints. Within this study 1.3-1.4 improvement in fatigue strength was found for the both PWT methods; and
- ENS method with r_{ref} = 0.05 mm and FAT630 for thin-walled structures seemed to be applicable to assess fatigue strength of such structures with the R = -1 loading.

References

Akita, M., Uematsu, Y., Kakiuchi, T., et al., Joint microstructures, mechanical properties and fatigue behaviour of ferritic stainless steel SUS 430 welds with different filler metals. *Weld. Int.*, 32, 427–435, 2018.

Björk, T., Mettänen, H., Ahola, A., et al., Fatigue strength assessment of duplex and super-duplex stainless steels by 4R method. *Weld. World*, 62, 1285–1300, 2018.

EN 10088-2, *Stainless steels - Part 2: Technical delivery conditions for sheet/plate and strip of corrosion resisting steels for general purposes*, European Committee for Standardization, 2014

EN ISO 14343, *Welding consumables - Wire electrodes, strip electrodes, wires and rods for arc welding of stainless and heat resisting steels – Classification*, European Committee for Standardization, 2017

European Commission, *Improving the fatigue performance of welded stainless steels*. Final report for contract No 7210-PR/303, 2007

Haagensen, P. J., Maddox S. J., *IIW Recommendations on Post Weld Improvement of Steel and Aluminium Structures*. IIW-document XIII-2200r7-07, 2010

Hobbacher, A., *Recommendations for Fatigue Design of Welded Joints and Components*, 2nd edn., Springer International Publishing, Cham, 2016

Maddox, S. J., Manteghi, S., Fatigue tests on duplex stainless steel tubular T-joints, *Weld. World*, 46, 12–19. 2002

Niemi, E., Koskimäki, M., Fatigue strength of welded joints in three types of stainless steel, *Weld. World*, 39, 65–73, 1997

Packer, J. A., Wardenier, J., Zhao, X. L., et al., *Design Guide for Rectangular Hollow Section (RHS) Joints Under Predominatly Static Loading*, CIDECT, LSS Verlag, 2009

Skriko, T., Ghafouri, M., Björk, T., Fatigue strength of TIG-dressed ultra-high-strength steel fillet weld joints at high stress ratio, *Int. J. Fatigue*, 94, 110–120, 2017

Sonsino, C. M., Fricke, W., De Bruyne, F., et al., Notch stress concepts for the fatigue assessment of welded joints - Background and applications. *Int. J. Fatigue*, 34, 2–16, 2012

van Wingerde, A. M., The fatigue behaviour of T- and X-joint made of square hollow sections, *Heron*, 37, 1–182, 1992

Yıldırım, H. C., Recent results on fatigue strength improvement of high-strength steel welded joints. *Int. J. Fatigue*, 101, 408–420, 2017